Journal of Biomedical Optics

SPIEDigitalLibrary.org/jbo

Clinical Raman measurements under special ambient lighting illumination

Jianhua Zhao
Michael Short
Thomas Braun
Harvey Lui
David McLean
Haishan Zeng

SPIE

Journal of Biomedical Optics 19(11), 111609 (November 2014)

TECHNICAL NOTE

Clinical Raman measurements under special ambient lighting illumination

Jianhua Zhao,[a,b] Michael Short,[a] Thomas Braun,[c] Harvey Lui,[b] David McLean,[b] and Haishan Zeng[a,b,*]
[a]British Columbia Cancer Research Center, Imaging Unit—Integrative Oncology Department,
675 West 10th Avenue, Vancouver, BC V5Z 1L3, Canada
[b]University of British Columbia and Vancouver Coastal Health Research Institute, Photomedicine Institute,
Department of Dermatology and Skin Science, Vancouver, BC V5Z 4E8, Canada
[c]Verisante Technology Inc., Vancouver, BC V6M 2A3, Canada

Abstract. One challenge in facing the application of biomedical Raman spectroscopy is that the Raman signal is acquired in a dark operation room. It is inconvenient for both the operator and the patient because it is difficult for the operator to accurately and precisely locate the target in the dark environment, and the patient feels uncomfortable in such a setting. In this note, we propose a method to implement biomedical Raman measurement with an illumination source, by multiple filtering of the illumination and the collection optics. Experimental results are demonstrated on skin Raman measurement under 785-nm excitation. [DOI: 10.1117/1.JBO.19.11.111609]

Keywords: Raman spectroscopy; illumination spectral shaping; light-emitting diode illumination; multiple-filtering.

Paper 140130SSTNR received Feb. 28, 2014; revised manuscript received May 20, 2014; accepted for publication May 22, 2014; published online Jun. 17, 2014.

Raman spectroscopy is a vibrational spectroscopic technique that is more specific to molecules than other spectroscopic techniques such as reflectance or fluorescence. But because the Raman signal of tissue is intrinsically weak, it previously required long integration times to acquire a single Raman spectrum. With technical advancements, the integration time has been reduced to <1 s, paving the way for translating the technique from the laboratory to a clinical setting.[1–4] The method has now been widely used for noninvasive *in vivo* investigation of skin cancers,[1–6] breast cancers,[7,8] cervical cancers,[9,10] lung cancers,[11,12] colon cancers,[13–15] gastric cancers,[16] and oral cancers.[17,18] For example, a recent large-scale clinical study carried out by our group demonstrated that real-time Raman spectroscopy can be used to distinguish malignant from benign skin lesions with sensitivity of 90% and specificity of 66%.[3] However, one challenge facing the operator and patients is that either the Raman signal is acquired in a dark room environment or the ambient room light has to be completely blocked from entering the probe[18] because the ambient room light interferes with the Raman signals. However, the dark room environment is inconvenient for both the operator and the patient, and both methods make it difficult to precisely locate the target.

For traditional Raman spectrum measurement, the charge coupled device (CCD) dark-noise and ambient background are usually measured before every measurement and then are sequentially subtracted immediately after the CCD readout.[2] However, this procedure cannot completely remove the effect of an ambient light source because the amount that leaks into the Raman system depends on the position, angle of the probe, and varying shadows of moving subjects in a clinical setting. Another limiting factor of this approach is that the CCD dynamic range is limited. The ambient background will reduce the maximum signal that can be measured even if it can be completely subtracted. Another method to remove the ambient background is the shifted excitation Raman difference spectroscopy (SERDS).[19–22] In SERDS, the sample is excited with two wavelengths that are shifted by a few nanometers and the spectrum is the difference of the two measurements, where the ambient background is removed by subtraction. However, this technique also has a number of limitations: (1) The ambient signal may be different during the two measurements and thus complete removal is impossible; (2) The associated tissue fluorescence background may not be completely removed due to the photobleaching effect; (3) Because there are two measurements in quick succession in SERDS, the amount of energy delivered in each measurement has to be reduced to approximately half the maximum allowed for a single measurement for safety reasons. This restriction decreases the signal-to-noise ratio by twofold; (4) The maximum allowable Raman signal is reduced, which decreases the signal-to-noise ratio, because each detector has a limited dynamic range. Therefore, it is preferable to completely prevent the ambient light from entering into the system either in a traditional Raman or a SERDS measurement.

On this note, we present a method to implement Raman measurement under ambient illumination with visible light that is optically filtered of near infrared (NIR) wavelengths. Its application was demonstrated in skin Raman measurement under 785-nm excitation. The 785-nm laser is the most commonly used laser source for biomedical Raman applications. It has a number of advantages: (1) The light at this wavelength penetrates deeper into the tissue than shorter wavelengths; (2) the fluorescence background of tissue at this excitation wavelength is relatively weaker than shorter excitation wavelengths; and (3) the Raman quantum yield of the tissue at this excitation wavelength is higher than that of longer excitation wavelengths.

*Address all correspondence to: Haishan Zeng, E-mail: hzeng@bccrc.ca

The *in vivo* clinical Raman system demonstrated in this work has been reported elsewhere.[1,2] It is comprised of a 785-nm diode laser, a fiber delivery system, a hand-held probe, and a spectrograph and detector system. The 785-nm laser beam is delivered to the Raman probe through a 200-μm-core diameter single fiber and illuminates a 3.5-mm diameter skin area. The raw signal from the sample is collected by the probe and transmitted to the spectrometer through a fiber bundle for spectral analysis. The integrated software contains all calibration procedures and real-time data processing, including intensity calibration and fluorescence background removal according to the Vancouver Raman algorithm with a fifth-order polynomial fitting.[23] Such a system performs very well in a dark operating environment.[2]

In order to filter the ambient light, we investigated the spectral properties of a number of light sources that may be part of the ambient light during clinical Raman measurement, including indirect day light, fluorescent lamps, liquid crystal display (LCD) monitors, cathode ray tubes (CRT) monitors, light-emitting diode (LED) monitors, and many types of white LED lamps that are commercially available, including phosphor-based and red-green-blue (RGB) diode-based white LED lamps. Figure 1 shows the spectra of these sources, and for illustration purposes the spectra between 750 and 900 nm were amplified. It can be seen that all these sources have visible and NIR emissions. Day light, fluorescence lamps, LCD monitors, and CRT monitors have very sharp emission peaks in the Raman signal range (800 to 910 nm), which are very difficult if not impossible to completely remove once they begin leaking into the Raman system. In contrast to the above sources, LED monitors and white LED lamps have much weaker and smoother NIR emissions. It is expected that even if there is some leakage of an LED monitor or white LED lamp into the collection arm, these leaked signals may be removed the same way as tissue fluorescence background is removed.[23]

Figure 2 shows the Raman spectra of a palm skin when these sources act as ambient lighting. It can be seen that the daylight has a profound effect on the Raman spectrum because it has many absorption lines and emission peaks in the spectral range. The Raman spectrum of palm skin under indirect sunlight is significantly different from that of palm skin in the dark (no ambient light). The Raman spectrum of palm skin also shows a number of spurious peaks under fluorescent lamp or LCD monitor illumination (highlighted by arrows). The CRT monitor causes a spurious peak around 700 cm^{-1}. No obvious spurious peaks are identified under white LED lamp or LED monitor illumination.

As noted from Figs. 1 and 2, only white LED lamp and LED monitor as ambient illumination sources do not obviously interfere with the Raman measurements. However, these commercially available white LED-based light sources also have weak and smooth emissions in the NIR region as shown in Fig. 1. Therefore, a broad band-pass filter has to be used so that the visible light can be transmitted while the NIR emissions can be blocked. The long-pass filter in the signal collection path also has to be carefully designed so that the visible light can be rejected. Figure 3 shows the transmission properties of the multiple-filtering system, including the broad band-pass filter, the long-pass filter, and the narrow band-pass laser-line filter. The broad band-pass filter (FSR-BG39, Newport, California), placed in the LED light source, passes through all the visible light and blocks all the NIR light that is longer than 700 nm

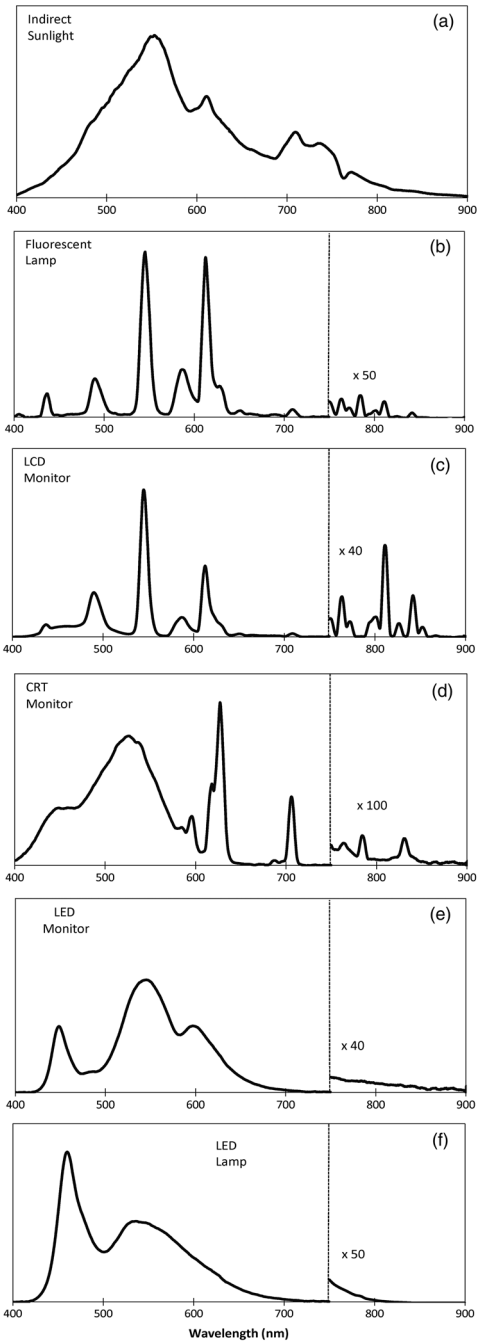

Fig. 1 Representative emission spectra of indirect sunlight (a), fluorescence lamp (b), liquid crystal display (LCD) monitor (c), cathode ray tubes (CRT) monitor (d), light-emitting diode (LED) monitor (e), and LED lamp (f) measured using an Ocean Optics spectrometer (USB400-VIS-NIR, Ocean Optics, Florida). Note that all these sources have emissions in the NIR range. The range 750 to 900 nm is amplified for illustration purpose.

for illumination. The long-pass filter (BLP01-785R-25, Semrock, New York), placed in the Raman signal collection path, blocks all the visible light and NIR light that is less than 785 nm, and passes through all the NIR light that is longer than 785 nm for the Raman spectrum measurement. Otherwise the visible component entering the spectrometer may generate second-order signals that will also interfere with the Raman signals. The narrow band-pass laser-line filter (LL01-785-12.5,

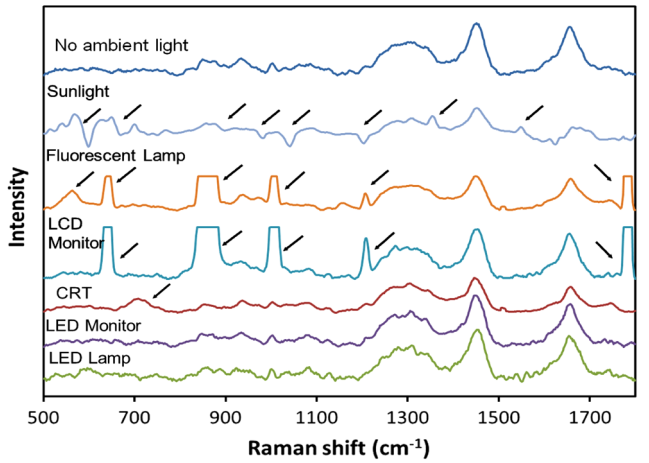

Fig. 2 Raman spectra of human palm skin in dark (no ambient lighting) and under indirect sunlight, fluorescence lamp, LCD monitor, CRT monitor, LED monitor, and LED lamp obtained with the *in vivo* clinical Raman system. The integration time is 1 s. The spurious peaks caused by the illumination lamps are highlighted by arrows. Strong spurious peaks are truncated and all spectra are shifted for illustration purpose.

Semrock, New York), placed in the Raman excitation path suppresses the laser side bands and emissions from within the fiber.

Figure 4 demonstrates the tested results of this design measured directly under a white LED lamp as the worst case scenario. Figure 4(a) shows the emission spectra of the LED light source with/without the designed broad band-pass filters. Figure 4(b) shows the LED light leaked into the Raman system with/without the broad band-pass filters. Note that without the designed broad band-pass filter, the emissions from the white LED lamp have weak signals in the NIR region that are leaked into the collection path [dashed line in Fig. 4(b)]. Although the NIR emission of the white LED lamps may be removed by the Vancouver Raman algorithm,[23] the effect is still profound as the dynamic range of the CCD detectors are limited. In an ideal situation, the NIR emissions of the white LED lamps

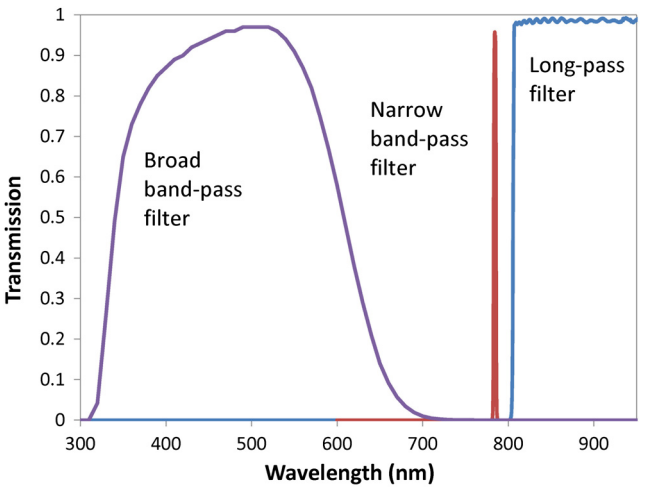

Fig. 3 Design of the multiple-filtering system. The broad band-pass filter is used to filter the illumination LED light source; the narrow band-pass filter is used to reject the side bands of the laser line and emissions from within the delivery fiber, and the long-pass filter is used to reject visible LED light source and laser line.

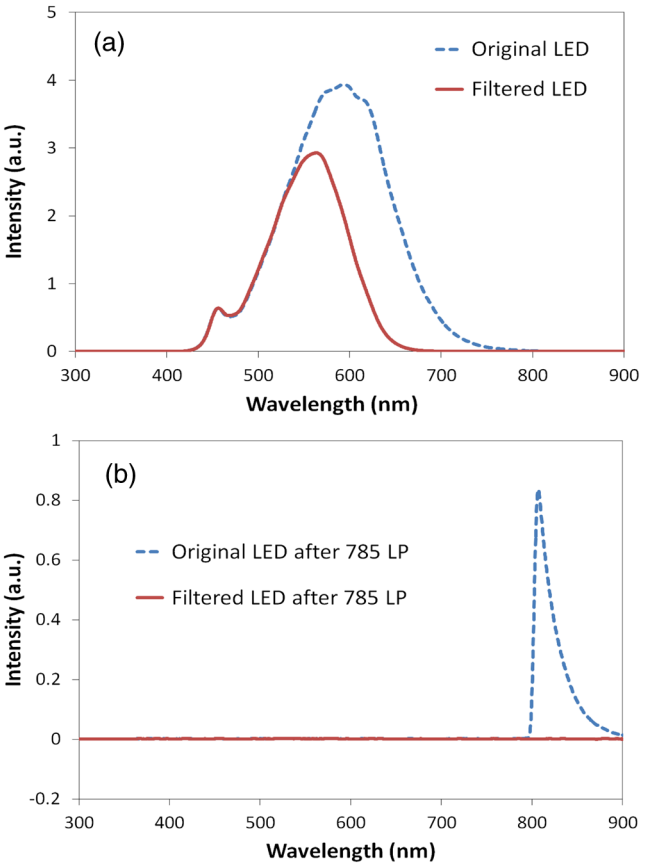

Fig. 4 Emission spectra of the white LED light source filtered with or without the designed filters (a) and the leaked LED light into the Raman signal collection path from the light source without and with the designed filters (b). Solid lines: with designed broad band-pass filters, dashed lines: without designed broad band-pass filters; LP: long pass filter. Note that the leaked LED light is completely blocked after applying the broad band-pass filter in (b).

should be completely blocked. With the designed broad band-pass filters, the NIR emission of the white LED lamp is sufficiently suppressed and there is no light leaked into the collection path [solid lines in Fig. 4(b)]. Therefore, by this design, the visible part of the white LED light passes through the broad band-pass filter for illumination [solid lines in Fig. 4(a)], whereas the NIR part is completely blocked from the Raman system [solid lines in Fig. 4(b)]. The filtered white LED illumination light and the laser light are completely blocked by the long-pass filter [solid lines in Fig. 4(b)].

Figure 5 shows the Raman spectra of a reflectance disk (SRS-99-020, Labsphere, North Sutton, New Hampshire) and palm skin *in vivo* with and without the multiple-filtered LED as ambient illumination. All the spectra are measured with an integration time of 1 s. We can see that there is essentially no difference between the two spectra of the reflectance disk with or without the designed LED illumination. Due to noise and biological variability, the two spectra of palm skin show trivial differences that are statistically insignificant based on an F-test of variance ($p = 0.4591$).

In summary, we proposed a method and designed a multiple-filtered LED-based light source for clinical Raman measurement. The critical components of the system are the filtered LED sources and the multiple-filters for the illumination and signal collection. Experimental results demonstrated that

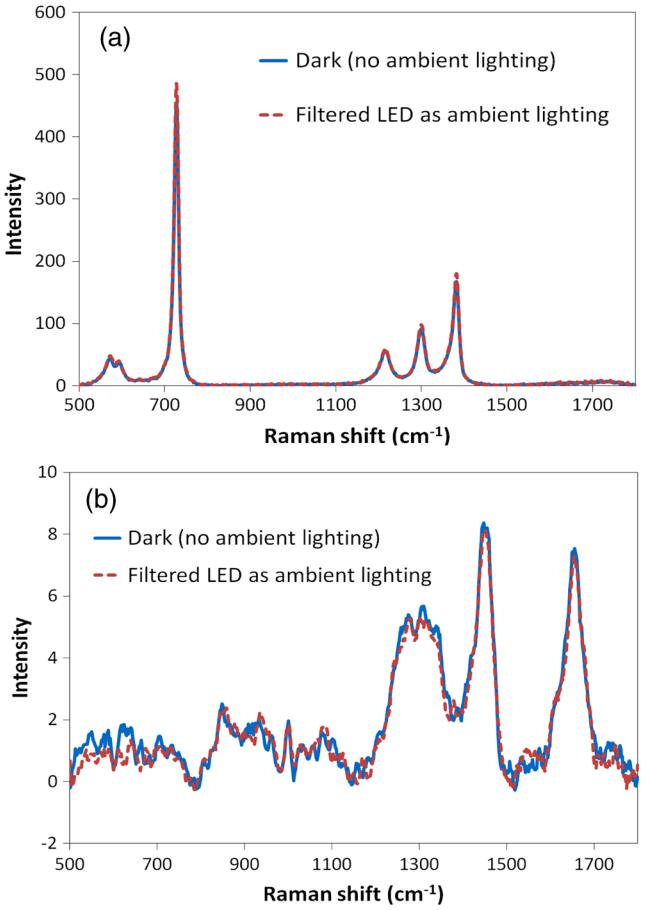

Fig. 5 Raman spectra of reflectance disk (a) and palm skin (b) with and without LED as ambient illumination at 1-s integration time. Solid lines: dark without ambient illumination, dashed lines: with multiple-filtered LED as ambient illumination.

clinical Raman spectrum could be measured in an illumination environment by the multiple-filtered light source without interference. The principle to implement Raman measurement with ambient illumination is that the emissions of the illuminating light source in the Raman wavelength-range should be completely blocked. The ambient illuminating light source should not be leaked into the signal collection path. We tested a number of light sources and found that only LED monitors and white LED light sources could be effectively filtered for the purpose of ambient illumination in clinical Raman measurement. The intensity of the filtered LED source is similar to that of a regular fluorescent lamp. It cannot be too intense so as not to generate side effects such as tissue fluorescence that bypasses the designed multiple filters. It can be placed on the ceiling or a table in the clinical room. There are no added complications or side effects for patients. With the same principle, a multiple-filtered LED light source can be used for other Raman measurement, such as guiding the probe in an endoscopic application.

Acknowledgments

This work is supported in part by the Canadian Dermatology Foundation (CDF), Canadian Institutes for Health Research (CIHR), and Verisante Technology Inc. Mr. Wei Zhang is acknowledged for his assistance in the measurement.

References

1. Z. Huang et al., "Rapid near-infrared Raman spectroscopy system for real-time in vivo skin measurements," *Opt. Lett.* **26**(22), 1782–1784 (2001).
2. J. Zhao et al., "Integrated real-time Raman system for clinical in vivo skin analysis," *Skin Res. Technol.* **14**(4), 484–492 (2008).
3. H. Lui et al., "Real-time Raman spectroscopy for in vivo skin cancer diagnosis," *Cancer Res.* **72**(10), 2491–2500 (2012).
4. J. T. Motz et al., "Real-time Raman system for in vivo disease diagnosis," *J. Biomed. Opt.* **10**(3), 031113 (2005).
5. N. S. Eikje, K. Aizawa, and Y. Ozaki, "Vibrational spectroscopy for molecular characterisation and diagnosis of benign, premalignant and malignant skin tumours," *Biotechnol. Ann. Rev.* **11**, 191–225 (2005).
6. C. A. Lieber et al., "In vivo nonmelanoma skin cancer diagnosis using Raman microspectroscopy," *Lasers Surg. Med.* **40**(7), 461–467 (2008).
7. J. Surmacki et al., "Raman imaging at biological interfaces: applications in breast cancer diagnosis," *Mol. Cancer* **12**, 48 (2013).
8. A. S. Haka et al., "Diagnosing breast cancer by using Raman spectroscopy," *Proc. Natl. Acad. Sci. U. S. A.* **102**(35), 12371–12376 (2005).
9. M. D. Keller et al., "Detecting temporal and spatial effects of epithelial cancers with Raman spectroscopy," *Dis. Markers* **25**(6), 323–337 (2008).
10. S. Duraipandian et al., "In vivo diagnosis of cervical precancer using Raman spectroscopy and genetic algorithm techniques," *Analyst* **136** (20), 4328–4336 (2011).
11. M. Short et al., "Development and preliminary results of an endoscopic Raman probe for potential in-vivo diagnosis of lung cancers," *Opt. Lett.* **33**(7), 711–713 (2008).
12. M. A. Short et al., "Using laser Raman spectroscopy to reduce false positives of autofluorescence bronchoscopies: a pilot study," *J. Thorac. Oncol.* **6**(7), 1206–1214 (2011).
13. M. A. Short et al., "Using high frequency Raman spectra for colonic neoplasia detection," *Opt. Express* **21**(4), 5025–5034 (2013).
14. E. Widjaja, W. Zheng, and Z. Huang, "Classification of colonic tissues using near-infrared Raman spectroscopy and support vector machines," *Int. J. Oncol.* **32**(3), 653–662 (2008).
15. R. Manoharan et al., "Laser-induced fluorescence spectroscopy of colonic dysplasia: prospects for optical histological analysis," *Proc. SPIE* **2388**, 417–422 (1995).
16. S. K. Teh et al., "Near-infrared Raman spectroscopy for early diagnosis and typing of adenocarcinoma in the stomach," *Br. J. Surg.* **97**(4), 550–557 (2010).
17. K. Guze et al., "Parameters defining the potential applicability of Raman spectroscopy as a diagnostic tool for oral disease," *J. Biomed. Opt.* **14** (1), 014016 (2009).
18. K. Guze et al., "Pilot study: Raman spectroscopy in differentiating premalignant and malignant oral lesions from normal mucosa and benign lesions in humans," *Head Neck* (2014).
19. P. Shreve, N. J. Cherepy, and R. A. Mathies, "Effective rejection of fluorescence interference in Raman spectroscopy using a shifted excitation difference technique," *Appl. Spectrosc.* **46**(4), 707–711 (1992).
20. J. Zhao, M. M. Carrabba, and F. S. Allen, "Automated fluorescence rejection using shifted excitation Raman difference spectroscopy," *Appl. Spectrosc.* **56**(7), 834–845 (2002).
21. P. A. Mosier-Boss, S. H. Lieberman, and R. Newbery, "Fluorescence rejection in Raman spectroscopy by shifted-spectra, edge detection, and FFT filtering techniques," *Appl. Spectrosc.* **49**(5), 630–638 (1995).
22. P. Matousek, M. Towrie, and A. Parker, "Simple reconstruction algorithm for shifted excitation Raman difference spectroscopy," *Appl. Spectrosc.* **59**(6), 848–851 (2005).
23. J. Zhao et al., "Automated autofluorescence background subtraction algorithm for biomedical Raman spectroscopy," *Appl. Spectrosc.* **61** (11), 1225–1232 (2007).

Biographies of the authors are not available.